

## ARTICLE



# B1-cell-produced anti-phosphatidylserine antibodies contribute to lupus nephritis development via TLR-mediated Syk activation

Kongyang Ma<sup>1,2,3</sup>, Wenhan Du<sup>2,4</sup>, Shiyun Wang<sup>2</sup>, Fan Xiao<sup>2</sup>, Jingyi Li<sup>5</sup>, Jie Tian<sup>6</sup>, Yida Xing<sup>7</sup>, Xiaodan Kong<sup>7</sup>, Ke Rui<sup>6</sup>, Rencai Qin<sup>1</sup>, Xiaoxia Zhu<sup>8</sup>, Jing Wang<sup>9</sup>, Cainan Luo<sup>10</sup>, Haijing Wu<sup>11</sup>, Yun Zhang<sup>12</sup>, Chengping Wen<sup>12</sup>, Lan He<sup>9</sup>, Dongzhou Liu<sup>3</sup>, Hejian Zou<sup>8</sup>, Qianjin Lu<sup>11</sup>, Lijun Wu<sup>10</sup> and Liwei Lu<sup>2,4,13</sup>

© The Author(s), under exclusive licence to CSI and USTC 2023

Autoantibodies produced by B cells play a pivotal role in the pathogenesis of systemic lupus erythematosus (SLE). However, both the cellular source of antiphospholipid antibodies and their contributions to the development of lupus nephritis (LN) remain largely unclear. Here, we report a pathogenic role of anti-phosphatidylserine (PS) autoantibodies in the development of LN. Elevated serum PS-specific IgG levels were measured in model mice and SLE patients, especially in those with LN. PS-specific IgG accumulation was found in the kidney biopsies of LN patients. Both transfer of SLE PS-specific IgG and PS immunization triggered lupus-like glomerular immune complex deposition in recipient mice. ELISPOT analysis identified B1a cells as the main cell type that secretes PS-specific IgG in both lupus model mice and patients. Adoptive transfer of PS-specific B1a cells accelerated the PS-specific autoimmune response and renal damage in recipient lupus model mice, whereas depletion of B1a cells attenuated lupus progression. In culture, PS-specific B1a cells were significantly expanded upon treatment with chromatin components, while blockade of TLR signal cascades by DNase I digestion and inhibitory ODN 2088 or R406 treatment profoundly abrogated chromatin-induced PS-specific IgG secretion by lupus B1a cells. Thus, our study has demonstrated that the anti-PS autoantibodies produced by B1 cells contribute to lupus nephritis development. Our findings that blockade of the TLR/Syk signaling cascade inhibits PS-specific B1-cell expansion provide new insights into lupus pathogenesis and may facilitate the development of novel therapeutic targets for the treatment of LN in SLE.

**Keywords:** B1 cell; Anti-phosphatidylserine antibodies; Lupus nephritis; TLR; Syk

*Cellular & Molecular Immunology* (2023) 20:881–894; <https://doi.org/10.1038/s41423-023-01049-2>

## INTRODUCTION

Systemic lupus erythematosus (SLE) is a chronic autoimmune disease with multiple organ involvement, in which T and B cells play a central role in driving autoimmune pathogenesis during disease progression. Many studies, including our recent findings, have shown that proinflammatory cytokines and effector T cells, especially Th17 and T follicular helper cells, are critically involved in promoting germinal center reaction, plasma cell formation and autoantibody production [1–3]. A hallmark of SLE is the

production of autoantibodies against cellular components, including nuclear antigens. Among the identified autoantibodies in lupus patients, anti-dsDNA antibodies are the most studied for their clinical importance in disease activity and lupus nephritis (LN) progression in SLE patients, but increasing evidence indicates that anti-dsDNA antibodies alone may not be sufficient to initiate lupus nephritis development [4, 5]. Thus, it remains to be investigated whether other autoantibodies are directly involved in renal damage during lupus development. Antiphospholipid

<sup>1</sup>Centre for Infection and Immunity Studies, School of Medicine, The Sun Yat-sen University, Shenzhen 518107 Guangdong, China. <sup>2</sup>Department of Pathology and Shenzhen Institute of Research and Innovation, The University of Hong Kong, Hong Kong 999077, China. <sup>3</sup>Department of Rheumatology, Shenzhen People's Hospital, The Second Clinical Medical College, Jinan University, Shenzhen, China. <sup>4</sup>Chongqing International Institute for Immunology, Chongqing 400038, China. <sup>5</sup>Department of Rheumatology and Immunology, Southwest Hospital, The First Hospital Affiliated to Army Medical University, Chongqing 400038, China. <sup>6</sup>Department of Laboratory Medicine, Affiliated Hospital and Institute of Medical Immunology, Jiangsu University, Zhenjiang, China. <sup>7</sup>Department of Rheumatology, The Second Affiliated Hospital of Dalian Medical University, Dalian, China. <sup>8</sup>Department of Rheumatology, Huashan Hospital, Fudan University, Shanghai, China. <sup>9</sup>Department of Rheumatology and Immunology, The First Affiliated Hospital of Xi'an Jiaotong University, Xi'an 710061 Shaanxi, China. <sup>10</sup>Department of Rheumatology and Immunology, People's Hospital of Xinjiang Uygur Autonomous Region, Urumqi, China. <sup>11</sup>Department of Dermatology, Hunan Key Laboratory of Medical Epigenomics, Second Xiangya Hospital, Central South University, Changsha, Hunan, China. <sup>12</sup>Key Laboratory of Chinese Medicine Rheumatology of Zhejiang Province, Institute of Basic Research in Clinical Medicine, College of Basic Medical Science, Zhejiang Chinese Medical University, Hangzhou 310053, China. <sup>13</sup>Centre for Oncology and Immunology, Hong Kong Science Park, Hong Kong, China. ✉email: qianlu5860@pumcdern.cams.cn; wwlj330@163.com; liweilu@hku.hk

Received: 31 January 2023 Accepted: 22 May 2023

Published online: 9 June 2023

antibodies have been identified in several autoimmune and infectious diseases, such as SLE, primary antiphospholipid syndrome, systemic sclerosis, malaria and viral infections [6–8]. The prevalence of antiphospholipid antibodies (aPL), including autoantibodies against  $\beta_2$ -glycoprotein I ( $\beta_2$ GPI), cardiolipin and prothrombin, is associated with thrombosis, pregnancy complications, and neurological disorders in SLE patients [7, 9, 10]. Recent studies have also reported a novel endosomal lysobisphosphatidic acid (LBPA) as an immunogenic phospholipid antigen for inducing thrombosis and autoimmune pathology [11]. Currently, it is not clear whether antiphospholipid antibodies contribute to the development of LN in SLE.

As one of the most severe manifestations in SLE patients, LN is initiated by renal immune-complex deposition and lymphocytic infiltration [12]. In SLE patients, the levels of phosphatidylserine (PS)-specific phospholipase A1 and anti-PS antibodies are elevated and involved in lupus progression with multiple immunomodulatory effects [13, 14]. However, it is unclear which B-cell subsets produce anti-PS antibodies and whether anti-PS antibodies contribute to tissue damage and nephropathy during SLE development.

B1 cells are divided into a major CD5<sup>+</sup> B1a subset and a minor CD5<sup>-</sup> B1b subset in mice [15]. Compared with conventional B2 cells, B1 cells are critically involved in antiviral response and immune tolerance breakdown [16–19]. Several studies have reported that B1 cells accumulate in damaged kidneys and contribute to autoantibody production in lupus model mice [18, 19]. Interestingly, B1 cells are found to secrete dsDNA-specific IgG and initiate autoimmune diabetes at the early stage in 4-week-old NOD mice [20]. Based on the major functional features of murine B1 cells, including spontaneous IgM secretion, T-cell activation and distinct transcriptomic profiles, human B1 cells have been previously identified with a phenotype of CD20<sup>+</sup>CD27<sup>+</sup>CD43<sup>+</sup>CD70<sup>-</sup> [21]. In particular, a small CD11b<sup>+</sup> human B1-cell subpopulation is considerably expanded with the potent capacity to stimulate T cells in SLE patients [22]. Although available evidence indicates a role of B1 cells in lupus pathogenesis, further studies are needed to determine if autoantibodies are produced by B1 cells and their involvement in the disease progression of SLE patients. We have recently identified a role of Toll-like receptor (TLR) signaling in maintaining the autoreactive plasma cell response in SLE, indicating the involvement of TLR signaling in controlling the functions of multiple B-cell subsets during lupus development [23, 24]. However, it remains to be investigated how TLR signaling regulates antibody production through B1 cells during lupus pathogenesis.

Here, we show the positive correlations of elevated anti-PS IgG levels with nephritis development and disease activity index in SLE patients and lupus model mice. Injection of purified PS-specific IgG from SLE serum samples triggered renal damage in recipient mice. Notably, immunization with PS triggered lupus-like syndromes in mice, indicating an important role of the PS-specific autoimmune response. Moreover, B1 cells were identified as the main cellular source of PS-specific IgG production in both lupus model mice and SLE patients. Moreover, inhibition of the TLR/Syk signaling pathway profoundly suppressed PS-specific B1-cell expansion and PS-specific IgG production. Overall, our findings provide new insight into the effector mechanisms of the B1-cell-mediated autoimmune response in nephritis progression during SLE development.

## METHODS

### Mice and treatment

Female MRL/MpJ-Fas<sup>lpr</sup>/J (MRL/Lpr) mice, control MRL/MPJ mice, C57BL/6J mice, and NOD Cg-Prkdc<sup>scid</sup>Il2rg<sup>tm1Wjl</sup>/SzJ (NSG) mice were purchased from The Jackson Laboratory (Bar Harbor, ME, USA). All mice were maintained at the Laboratory Animal Unit of the University of Hong Kong. All animal experiments were approved by the Committee on the Use of Live Animals in Teaching and Research (CULATR, No: 3392-14) at the University of Hong Kong.

Female NSG mice were intravenously (i.v.) injected with total serum from healthy donors (0.2 mg/mouse), SLE serum positive for PS-specific IgG (0.2 mg/mouse) or purified PS-specific IgG antibody from SLE serum (0.2 mg/mouse). Human autoantibody levels and human IgG deposition in the kidney were assessed 60 days after the first injection in mice.

For PS immunization, female C57 mice were subcutaneously (s.c.) immunized with (0.2 mg) phosphatidylserine (PS) liposomes in complete Freund's adjuvant (CFA, InvivoGen, San Diego, CA, USA) at day 0, and then s.c. injected with PS liposomes in incomplete Freund's adjuvant (IFA, InvivoGen) at days 14 and 28 to enhance the antigen-specific humoral response. Mice immunized with phosphocholine (PC) liposomes emulsified in adjuvants were used as controls. PS liposomes (PS:PC at 1:3) and PC liposomes were generated as previously described [25]. For peritoneal B1a cell depletion by hypotonic shock, we repeatedly intraperitoneally (i.p.) injected distilled water (0.5 ml for 4- to 8-week ages and 1 ml for more than 8-week ages) in female MRL/Lpr mice [20]. Sorted and purified  $1 \times 10^6$  PS-specific B1a cells and PS-nonspecific B1a cells from the peritoneal cavities of 24-week-old MRL/Lpr mice were then adoptively transferred into 6-week-old MRL/Lpr recipients by tail vein injection, and serum PS-specific IgG levels and renal damage were assessed at 4 weeks post cell transfer. Lupus mice were immunized with chromatin prepared from apoptotic splenocytes as previously described [24].

### Human samples

All SLE patients without antiphospholipid syndrome (APS) included in the study fulfilled the American College of Rheumatology criteria for the classification of SLE [26]. In addition, kidney biopsy sections from lupus nephritis patients were obtained from Queen Mary Hospital. All experiments with human samples were approved by the Institutional Medical Ethics Committee of Army Medical University (Reference Number: 2016-77-tmmu) and Institutional Review Board of the University of Hong Kong/Hospital Authority Hong Kong Western Cluster (HKU/HA HKW IRB) (Reference Number: UW 16-342). Written permission was obtained from all subjects who participated in the study, including 18 healthy donors and 64 SLE patients. Detailed information on healthy donors, SLE patients with low levels of PS-specific IgG antibodies and SLE patients with high levels of PS-specific IgG antibodies, including number, sex, age and patient characteristics, is included in Supplementary Table 1.

For serum transfer, serum samples were pooled from three active SLE patients with high PS-specific IgG levels and used for SLE serum transfer experiments and PS-specific IgG purification. The PS-specific IgG antibody was purified with a BSA-PS (Cloud-Clone, China)-conjugated antibody purification and concentration kit (Abcam, UK). A BCA protein assay (Pierce™ BCA Protein Assay Kit, Thermo Fisher Scientific, Waltham, MA, USA) was conducted to quantify the protein levels of purified PS-specific IgG, healthy serum, and SLE serum.

### Cell culture

Mouse CD19<sup>+</sup>CD11b<sup>+</sup>CD5<sup>+</sup> B1a cells, CD19<sup>+</sup>CD11b<sup>+</sup>CD5<sup>-</sup> B1b cells, and CD19<sup>+</sup>CD11b<sup>+</sup>CD5<sup>-</sup> B2 cells were purified using the B220 B-cell isolation kit (Miltenyi Biotec, Bergisch Gladbach, Germany) and a BD FACSAria SORP cell sorter (Becton Dickinson, >95% purity). PS-specific B1a cells were then sorted with the PS-labeled biotin-streptavidin system. Sorted and purified B-cell subsets were cultured in RPMI 1640 medium supplemented with 10% fetal bovine serum, 1 mM sodium pyruvate, 50  $\mu$ M  $\beta$ -ME, and antibiotics. Chromatin components (CCs) were extracted from splenocytes stimulated with 5 ng/ml Con A for 72 h. The CCs CpG ODN 2395 (5'-tcg tcg ttt tcg gcg cgc gcc g-3') (InvivoGen), ODN 2088 (5'-tcc tgg cgg gga agt -3') (InvivoGen), negative control (5'-tcc tga gct tga agt -3') (InvivoGen) and the Syk inhibitor R406 (Selleck Chemicals, Houston, TX, USA) were added to the lupus B1a cell culture system for functional analysis.

Peripheral blood was collected in clotting tubes for serum preparation and in sodium-heparin tubes for peripheral blood mononuclear cell (PBMC) isolation. PBMCs from SLE patients were isolated by Lymphoprep (STEMCELL Technologies, Vancouver, BC, Canada). Human CD20<sup>+</sup>CD70<sup>-</sup>CD27<sup>-</sup>CD43<sup>-</sup> double-negative (DN) B cells, CD20<sup>+</sup>CD70<sup>-</sup>CD27<sup>+</sup>CD43<sup>-</sup> memory B cells, or CD20<sup>+</sup>CD70<sup>-</sup>CD27<sup>+</sup>CD43<sup>+</sup> B1 cells in SLE PBMCs were excluded using a BD FACSAria SORP cell sorter (Becton Dickinson, San Jose, CA, USA) for the generation of human PBMCs with B-cell subset depletion.

### Flow cytometric analysis

Single-cell suspensions from the spleen and kidney and peripheral blood samples of lupus model mice were prepared according to standard

methods, and erythrocytes were lysed with 0.14 M NH<sub>4</sub>Cl 20 mM Tris (pH 7.4). Murine kidney tissue was digested after perfusion with PBS, and renal-infiltrated leukocytes were separated using Percoll (Sigma-Aldrich, St Louis, MO, USA). For multicolor flow cytometric analysis, a Zombie Aqua fixable viability dye (BioLegend, San Diego, CA, USA) was added to exclude dead cells, and an Fc receptor binding inhibitor (BioLegend) was used to block nonspecific Fc-gamma receptor (FcγR)-mediated binding of antibodies. The single-cell suspensions were then stained with anti-CD45-Pacific blue (20-F11), anti-CD19-FITC (6D5), anti-B220-PE (RA3-6B2), anti-CD5-PE7 (53-7.3), anti-CD43-PE (S11), anti-CD19-PerCp-Cy5.5 (6D5), anti-IgM-APC (RMM-1), anti-CD11b-PE (M1/70), biotin-labeled PS (Echelon Biosciences, Inc., EBI, UT, USA), PE/Cy7-labeled streptavidin, anti-mouse CD86-PerCp (GL-1), anti-CXCR3-PerCp/Cy5.5 (CXCR3-173), anti-mouse CD138-APC/Cy7 (281-2) and the isotype-matched control antibody from BioLegend (USA) for mouse samples. Intracellular Blimp1 was stained with anti-Blimp1-APC (5E7) with a Transcription Factor Staining Buffer Set (eBioscience, San Diego, CA, USA) according to the manufacturer's instructions. The phosphorylation of Syk (Cell Signaling Technology (CST), Danvers, MA, USA, #2710) and total Syk (CST #13198) levels in B1a cells were detected using the BD Phosflow™ Kit (BD Biosciences, San Diego, CA, USA). PBMC single-cell suspensions were stained with the Zombie Aqua fixable viability dye (BioLegend) to exclude dead cells and an Fc receptor binding inhibitor (BioLegend). Then, PBMCs were stained with FITC anti-human CD70 (113-16), PE anti-human CD43 (CD43-10G7), PerCP/Cy5.5 anti-human CD19 (HIB19), Pacific blue anti-human CD20 (2H7), and APC anti-human CD27 (M-T271) from BioLegend. All flow cytometric data were acquired using a BD LSR Fortessa cytometer (BD Biosciences) and analyzed with FlowJo software (BD Biosciences).

### Immunofluorescence staining

For glomerular anti-PS IgG deposition, frozen sections of kidney biopsies were stained with biotin-PS (Echelon Biosciences Inc., Salt Lake City, Utah, USA), Alex Fluor 488-conjugated Streptavidin (BioLegend), PE-conjugated anti-human IgG (BioLegend, M1310G05) and APC-conjugated anti-human IgM (BioLegend, MHM-88).

For glomerular immune complex deposition, frozen sections of kidney tissue were stained with FITC-conjugated anti-mouse IgG (BioLegend, Poly4060) and PE-conjugated anti-mouse IgM (BioLegend, RMM-1) overnight at 4 °C. DNA was visualized using Hoechst (Invitrogen, Carlsbad, CA, USA). A score on a scale of 0–3 was assigned for both IgG and IgM deposition for quantification [24].

For renal B1a cell infiltration staining, human B1 cells in frozen kidney biopsy sections from patients with lupus nephritis were stained with FITC-conjugated anti-human CD20 (2H7), PE-conjugated anti-human CD43 (10G7), and APC-conjugated anti-human CD27 (O323). Mouse B1a cells in frozen kidney sections from MRP/Lpr mice were stained with FITC-conjugated anti-mouse CD19 (6D5), PE-conjugated anti-mouse CD5 (53-7.3), and APC-conjugated anti-mouse CD43 (S11). All antibodies were purchased from BioLegend. Sections were analyzed by fluorescence microscopy using a Zeiss LSM780 confocal microscope.

### ELISA

Human serum samples (1:100 dilution) and mouse serum samples (1:200 dilution) were collected to measure the anti-dsDNA and anti-phosphatidylserine (anti-PS) IgG levels accordingly. Briefly, 1 mg/ml BSA-PS antigen (Cloud-Clone) or fetal calf dsDNA antigen (Sigma, US) was coated in 96-well ELISA plates (Thermo Fisher Scientific) (100 μl/well) at 4 degrees centigrade overnight. After blocking with 0.5% gelatin and 0.5% BSA buffer, human serum samples (1:100 dilution) and mouse serum samples (1:200 dilution) were then added. Biotin anti-human IgG (Clone: G18-145, BD Pharmingen, San Diego, CA, USA) or biotin anti-mouse IgG (Clone: Poly4053, BioLegend) were then added as detection antibodies. The HRP-streptavidin (BioLegend) and TMB substrate set (BioLegend) were then added accordingly. All data were collected in a microplate absorbance reader (Tecan, Austria) at OD450 nm absorbance [7].

### Comparative ELISA

Serum samples from active SLE patients (1:100 dilution in 50 μl PBS, SLEDAI > 5) were incubated with 0, 10, 50, or 100 μg PS liposomes or control PC liposomes. Subsequently, the PS-specific IgG levels in incubated serum samples were measured according to the instructions and analyzed by a microplate absorbance reader (Tecan) at OD450 nm absorbance [27].

### Enzyme-linked immunosorbent assay (ELISpot)

For the ELISpot assay of PS-specific IgG-secreting cells in humans and mice, a 96-well filtration plate (Millipore, Billerica, MA, USA) was coated with 1 mg/ml phosphatidylserine-BSA antigen (Cloud-Clone) (100 μl/well) at 4 degrees centigrade and incubated overnight. Then, purified B-cell subsets (2000 cells per well) were cultured in antigen coating filtration plates for 48 h. Then, biotin anti-human IgG (Clone: G18-145, BD Pharmingen) and biotin anti-mouse IgG (Clone: Poly4053, BioLegend) were added as detection antibodies. AKP streptavidin (BD Biosciences) and NBT/BCIP substrate (Millipore) were used. Finally, PS-specific IgG-secreting cells were quantified. To measure and compare the antibody-secreting capacity of various B-cell subsets, we performed separate experiments using sorting-purified B1a, B1b and B2 cells from the peritoneal cavity of 10-week-old female MRL/Lpr mice in the ELISpot assay and measured the parameters, including the spot number as spot forming units (SFU) and the spot size as relative spot volume (RSV), using an IRIS reader (Mabtech, Sweden) [24].

### RNA extraction and quantitative PCR analysis

Total RNA samples from lupus B1a cells, B1b cells and B2 cells were prepared with the RNeasy Kit (Qiagen, Hilden, Germany) and reverse transcribed with SuperScript III First-Strand Synthesis SuperMix (Invitrogen). Real-time PCR was performed with an Applied Biosystems Prism 7900HT real-time PCR system (Applied Biosystems, Foster City, CA, USA). The PCR primers we used are described in our previous study [20]. Relative expression levels of transcripts were calculated via the  $2^{-\Delta\Delta CT}$  method.

### Histopathologic assessment

Paraffin sections of mouse kidney tissue were subjected to H&E staining according to the instructions (Beyotime Biotechnology, Shanghai, China). The pathological changes were assessed using the glomerular activity score [24].

### Statistical analysis

Data in this study are indicated as the mean ± the standard error of the mean (SEM). The violin plot and box plot show the distribution of all data points [28]. Comparisons between two groups were performed by two-tailed unpaired Student's *t* test in mice and nonparametric Mann–Whitney *U* test in humans. Comparisons among more than two groups were performed using one-way ANOVA followed by the Newman–Keuls test as indicated. Correlations were assessed with Spearman's correlation coefficient. Statistical analysis was performed using GraphPad Prism (GraphPad Software, CA, USA). A value of *p* less than 0.05 was considered statistically significant.

## RESULTS

### PS-specific autoimmune response contributes to lupus nephritis development

To elucidate whether the PS-specific humoral response is involved in lupus model mice, we measured PS-specific IgG levels and analyzed their major sources in lupus-prone MRL/Lpr mice and mice with chromatin-induced lupus [24]. Persistently elevated levels of serum PS-specific IgG were observed in MRL/Lpr mice from 4 weeks of age to at least 24 weeks of age (Fig. 1A, left panel). Interestingly, significantly increased levels of PS-specific IgG were also observed in the peritoneal lavage fluid (PLF) of 12-week-old MRL/Lpr mice compared with age-matched MRL/MPJ mice (Fig. 1A, right panel). Consistently, increased serum PS-specific IgG levels were found in chromatin-induced lupus model mice at 6, 12 and 24 weeks post lupus induction (Fig. 1B).

To further determine the pathogenic effects of the PS-specific autoimmune response in vivo, we immunized C57 mice with the PS antigen (Fig. 1C). The liposomal PS/phosphatidylcholine complex was prepared as a PS liposome antigen, while liposomal PC was used as a control. Notably, the competitive ELISA results showed that the PS antigen could effectively neutralize serum PS-specific IgG levels in SLE patients compared with those of healthy controls (Supplementary Fig. 1).

Serological analysis showed elevated levels of PS-specific IgG and dsDNA-specific IgG autoantibodies in PS-immunized mice compared with control mice (Fig. 1D). Interestingly, comparable levels of

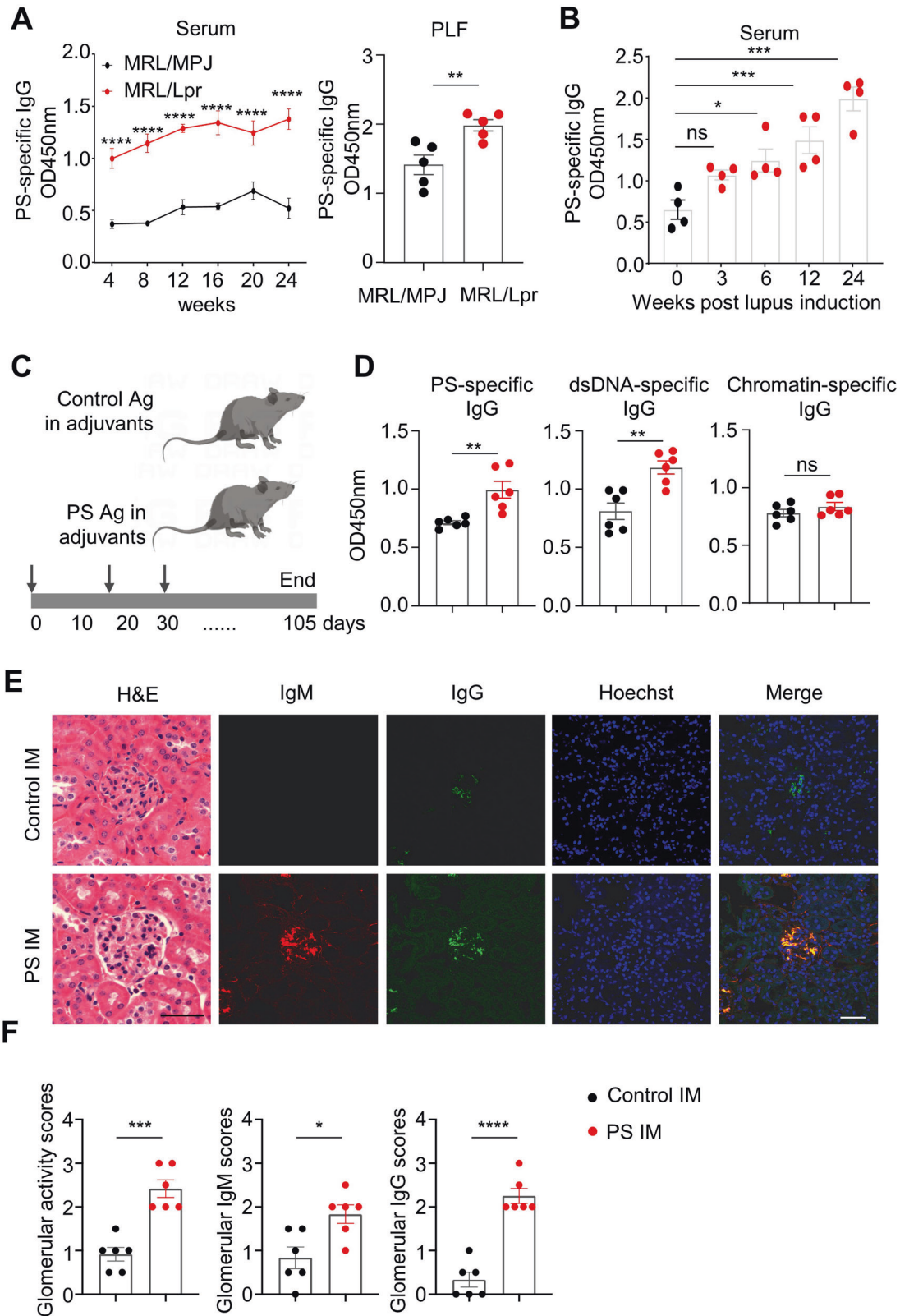


**Fig. 1** Pathogenic roles of PS-specific IgG in lupus model mice. **A** Representative data plots show PS-specific IgG in serum samples (1:200 dilution) of age-matched MRL/MPJ and MRL/Lpr mice at 4, 8, 12, 16, 20, and 24 weeks of age (left panel) and in peritoneal lavage fluid (PLF) samples at 12 weeks of age (right panel). **B** Data plot shows the PS-specific IgG levels in serum samples (1:200 dilution) of mice with chromatin-induced lupus at 0, 3, 6, 12, and 24 weeks ( $n = 4$  per group). **C** The schematic diagram shows the control or PS antigen (PS:PC = 1:3) immunization in mice. **D** Representative data plots show serum PS-specific IgG, dsDNA-specific IgG, and chromatin-specific IgG in serum samples (1:200 dilution) of control or PS-immunized mice for 12 weeks ( $n = 6$  per group). **E**, **F** Representative images and data plots show H&E staining, IgM, and IgG staining in kidney sections (scale bar, 20  $\mu\text{m}$ ) from control or PS-immunized mice for 12 weeks ( $n = 6$  per group). Unpaired two-tailed Student's *t* test, ns no significance; \* $p < 0.05$ ; \*\* $p < 0.01$ ; \*\*\* $p < 0.001$ ; \*\*\*\* $p < 0.0001$

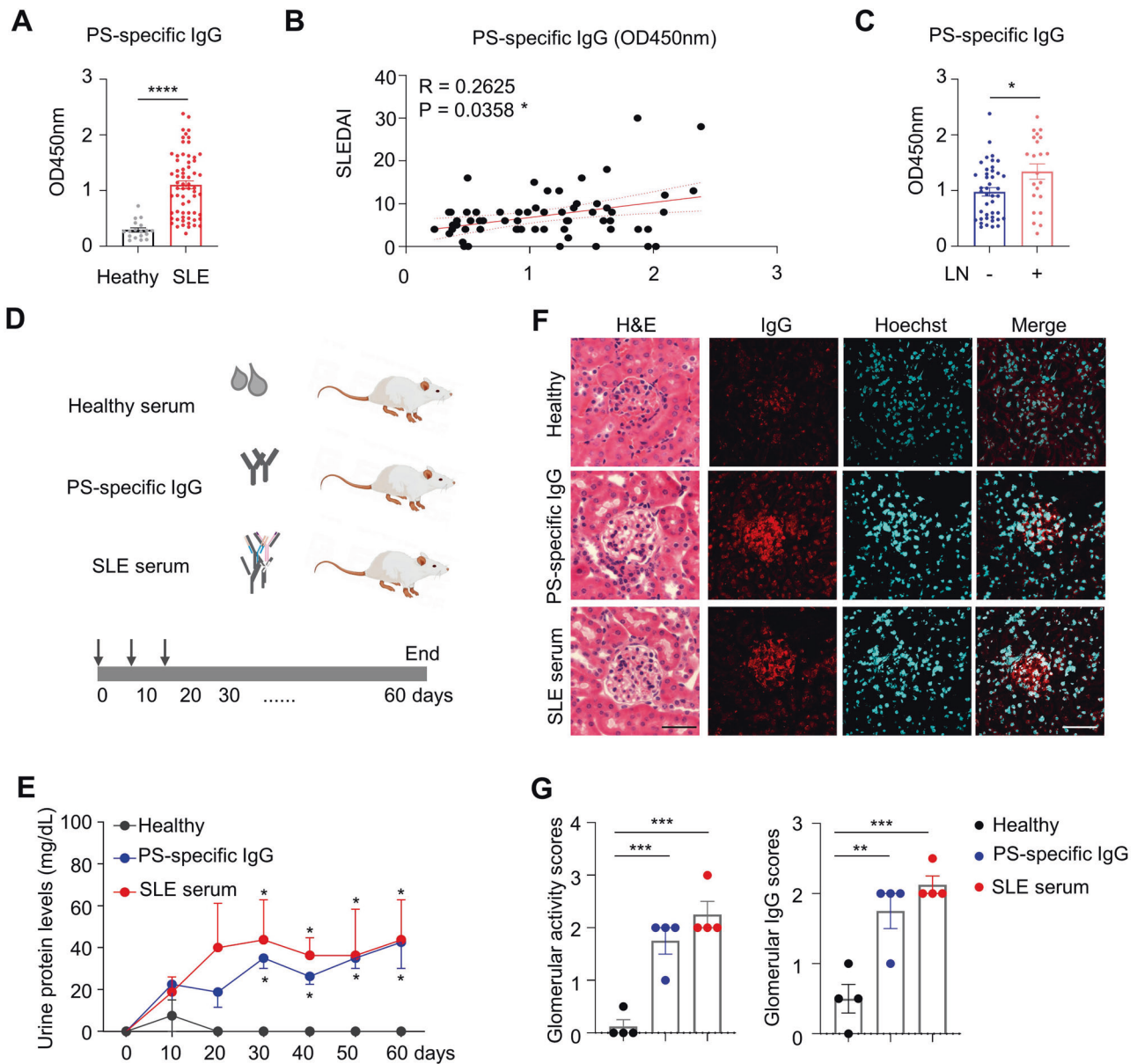


**Fig. 2** Pathogenic roles of PS-specific IgG in SLE patients. **A** Data plot showing serum levels of PS-specific IgG in healthy donors ( $n = 18$ ) and SLE patients ( $n = 64$ ). **B** Representative plot shows correlation analysis between SLEDAI scores and PS-specific IgG in SLE patients ( $n = 64$ ). **C** Data plot shows serum levels of PS-specific IgG in SLE patients with ( $n = 22$ ) and without lupus nephritis ( $n = 42$ ). **D** The schematic diagram shows the NSG mice injected with total serum (positive for PS-specific IgG) or purified PS-specific IgG from SLE patients ( $n = 4$  per group). **E** Plot shows the urine protein levels in NSG recipient mice at days 10, 20, 30, 40, 50 and 60 post serum transfer compared with those of the healthy group. **F, G** Representative images and plots show H&E staining and human IgG staining in kidney sections (scale bar, 20  $\mu$ m) from NSG recipients on day 60 post serum transfer ( $n = 4$  per group). Nonparametric Mann-Whitney  $U$  test (**A, C**), Spearman's rank correlation analysis (**B**) and one-way ANOVA (**E, G**); \* $p < 0.05$ ; \*\* $p < 0.01$ ; \*\*\* $p < 0.001$ ; \*\*\*\* $p < 0.0001$

chromatin-, muscarinic 3 receptor (M3R)- or collagenase II (CII)-specific IgG antibodies in serum were observed between PS-immunized mice and controls (Fig. 1D and Supplementary Fig. 2), indicating the specificity of the PS-specific autoimmune response in vivo. Moreover, compared with control mice, PS-immunized mice exhibited extensively increased renal damage and glomerular immune complex deposition at 12 weeks postimmunization (Fig. 1E, F). These results indicated a pathogenic role of PS antigen during lupus progression.

#### PS-specific IgG levels are significantly elevated and associated with nephritis development in SLE patients

To examine serum phosphatidylserine (PS)-specific IgG levels in SLE patients, we performed a serologic analysis using the serum

from healthy controls and SLE patients with or without lupus nephritis. As shown in Fig. 2A, PS-specific IgG levels were markedly increased in SLE patients. Elevated serum PS-specific IgG levels in SLE patients were further confirmed using the serial dilution method (1:100–1:1800) (Supplementary Fig. 3). A cohort study showed a positive correlation between the SLE disease activity index (SLEDAI) and PS-specific IgG levels in patients with SLE (Fig. 2B). Moreover, serological analysis also showed a strong positive correlation between serum dsDNA-specific IgG and PS-specific IgG levels in patients (Supplementary Fig. 4). Our cohort studies revealed significantly higher serum PS-specific IgG levels in SLE patients with nephritis than in those without lupus nephritis (Fig. 2C).

We then divided the SLE patients into two groups (high PS-specific IgG and low PS-specific IgG groups) using the mean value of PS-specific IgG levels in the SLE cohort. By analyzing the patient demographics and characteristics, we observed that SLE patients with high serum PS-specific IgG levels exhibited longer disease durations and higher SLEDAI and serum dsDNA-specific IgG levels than SLE patients with low serum PS-specific IgG levels. No significant differences in serum levels of C3 and C4 or white blood cell, platelet and red blood cell counts were observed between SLE patients with high PS-specific IgG and low PS-specific IgG levels (Supplementary Table 1). Notably, confocal microscopic examination of glomerular fluorescent intensity using PS-biotin, anti-IgM, and anti-IgG showed the colocalized pattern in the glomeruli of lupus nephritis patients, indicating the deposition of PS-reactive IgM and IgG in the kidney (Supplementary Fig. 5).

To determine if PS-specific IgG plays a pathogenic role during lupus development, PS-specific IgGs in SLE serum were purified with the PS-binding column and then intravenously transferred into immune-deficient NSG mice, while homologous total sera from SLE patients were injected as positive controls and serum from healthy individuals was injected as negative controls (Fig. 2D). The urine protein levels were assessed in NSG recipients. Persistently increased urine protein levels were observed in total SLE serum- and PS-specific IgG-injected recipient mice compared with healthy serum-injected controls from day 30 to 60 (Fig. 2E). On day 60 after the first injection, NSG recipient mice with PS-specific IgG or SLE serum injection showed significant glomerular activation and pronounced human IgG deposition in the kidneys (Fig. 2F, G), indicating a pivotal role of PS-specific IgG in driving renal damage during lupus nephritis development.

### B1 cells are the main source for PS-specific IgG production in lupus mice

To further determine the major pathogenic B-cell subsets responsible for the augmented PS-specific humoral response, we examined B1a, B1b and conventional B2 cells from the peritoneal cavities of mice by flow cytometric analysis. In mice immunized with PS, the absolute numbers of peritoneal B1a cells and B1b cells showed approximately four- to fivefold expansion compared with those in control mice (Fig. 3A). Interestingly, peritoneal B cells, rather than splenic B cells, predominantly secreted PS-specific IgG in lupus model mice. Moreover, PS-specific IgG-secreting B cells exhibited an ~2-fold higher abundance than dsDNA-specific IgG-secreting B cells (Supplementary Fig. 6).

To examine the major cellular source of PS-specific IgG secretion by B-cell subsets, we purified B1a, B1b and B2 cells from MRL/Lpr mice at 10 weeks of age (sorting purity is shown in Supplementary Fig. 7). The total IgG and PS-specific IgG-secreting cells were examined by ELISPOT assay using the spot number or Spot Forming Units (SFU) and the spot size as Relative Spot Volume (RSV) as parameters. As shown in Supplementary Fig. 8, the spot numbers (SFU) of total IgG in lupus B1a and B1b cells were significantly higher than those in the B2 cell subset. In particular, lupus B1a cells showed the highest SFU values of PS-specific IgG spots. The ratio of total IgG/PS-specific IgG SFU values represented the contribution of PS-specific IgG-secreting cells among total IgG-secreting cells. B1a cells also showed the highest ratio of PS-specific IgG-secreting cells in the peritoneal cavity of lupus model mice. Notably, the sum RSV values represented the total antibody-secreting capacity in B-cell subsets. Consistently, the sum RSV values of total IgG in lupus B1a and B1b cells were significantly higher than those from the B2 cell subset, among which lupus B1a cells showed the highest sum RSV values of PS-specific IgG spots. Overall, these results indicated that lupus B1a cells dominantly produced large amounts of PS-specific IgG when normalized to total IgG-secreting cells.

To examine the dynamic changes in anti-PS IgG-secreting B1 cells during lupus progression, we prepared sorting-purified

B1a, B1b, and B2 cell subsets from lupus model mice during disease onset (6 weeks old) and progressive (24 weeks old) stages for PS-specific ELISPOT detection. Lupus B1a cells from 6-week-old and 24-week-old MRL/Lpr mice dominantly produced PS-specific IgG. Importantly, lupus B1a cells were found to have ~2-fold and 4-fold higher levels of anti-PS IgG-secreting cells than B1b cells and B2 cells at 6 and 24 weeks of age, respectively (Fig. 3B).

Similarly, we also found that the proportion of B1a cells gradually increased in lupus-prone MRL/Lpr mice during the disease onset (6-week-old) and progressive (24-week-old) stages. As shown in Fig. 3C, significant expansion of B1a cells was observed in the peritoneal cavities and kidneys of 24-week-old MRL/Lpr mice. Notably, the number of renal-infiltrated B1a cells persistently increased from the disease onset stage when compared with age-matched MRL/MPJ controls. Moreover, the accumulated infiltration of CD43<sup>+</sup>CD5<sup>+</sup> B1a cells and CD43<sup>-</sup>CD5<sup>+</sup> B1b cells was confirmed in kidney sections of 24-week-old MRL/Lpr mice by confocal microscopy (Supplementary Fig. 9).

### B1-cell depletion attenuates the PS-specific autoimmune response and disease progression in lupus model mice

To determine whether the B1-cell-derived PS-specific autoimmune response is involved in the development of lupus, we induced intraperitoneal hypotonic shock in early-aged MRL/Lpr mice (4 weeks old) for B1-cell depletion as previously reported [20]. The efficacy of B1-cell depletion is shown in Supplementary Fig. 10. B1-cell depletion markedly reduced serum PS-specific IgG levels compared with those in control PBS-treated MRL/Lpr mice (Fig. 3D). Remarkably, representative images of renal sections showed reduced glomerular damage and immune complex deposition in B1-cell-depleted MRL/Lpr mice (Fig. 3E, F). Overall, our results indicated the key roles of the B1-cell-derived PS-specific autoimmune response in target organ damage during lupus development.

### B1 cells are the major source of PS-specific IgG in SLE patients

To determine the major source of PS-specific IgG in SLE patients, we generated B-cell subset-depleted (DN) PBMCs via electronic cell sorting. Notably, double-negative (DN) B subsets (CD27<sup>-</sup>CD43<sup>-</sup>), memory B cells (CD27<sup>+</sup>CD43<sup>-</sup>) or B1 cells (CD27<sup>+</sup>CD43<sup>+</sup>) were excluded in active SLE PBMCs and then plated for PS-specific IgG spot detection (Fig. 4A). Consistent with the findings in lupus model mice, B1-cell-depleted SLE PBMCs exhibited the least number of PS-specific IgG spots when compared with total SLE PBMCs, DN B-cell-depleted, or memory B-cell-depleted PBMCs (Fig. 4B).

Histopathological examination by immunofluorescence staining and confocal microscopy detected clusters of CD20<sup>+</sup>CD43<sup>+</sup>CD27<sup>+</sup> B1 cells in renal biopsies from lupus patients with diffuse proliferative LN (Class IV) (Fig. 4C). Statistical analysis showed significantly increased renal-infiltrated B1-cell levels within Class IV LN patients compared with Class II and III LN patients (Fig. 4D). Moreover, the levels of renal-infiltrated B1 cells were positively correlated with urine protein levels in LN patients (Fig. 4E).

### PS-specific B1 cells accelerate renal damage in lupus model mice

To further explore the direct effects of PS-specific B1 cells in lupus, we directly labeled PS-specific B1 cells with a PS-conjugated biotin-streptavidin system. Remarkably, more than 50% of the peritoneal PS-specific B cells were B1a cells in 24-week-old MRL/Lpr mice (Supplementary Fig. 11). The total number of PS-specific B1a cells exhibited a 2-fold increase in the peritoneal cavity, whereas the proportion of PS-specific B1a cells showed a marked 9-fold increase in renal tissue when compared with that in the renal tissue of age-matched MRL/MPJ controls (Fig. 5A).

Further examination of PS-specific B cells revealed that PS-specific IgG-secreting cells were enriched in sorting-purified PS-

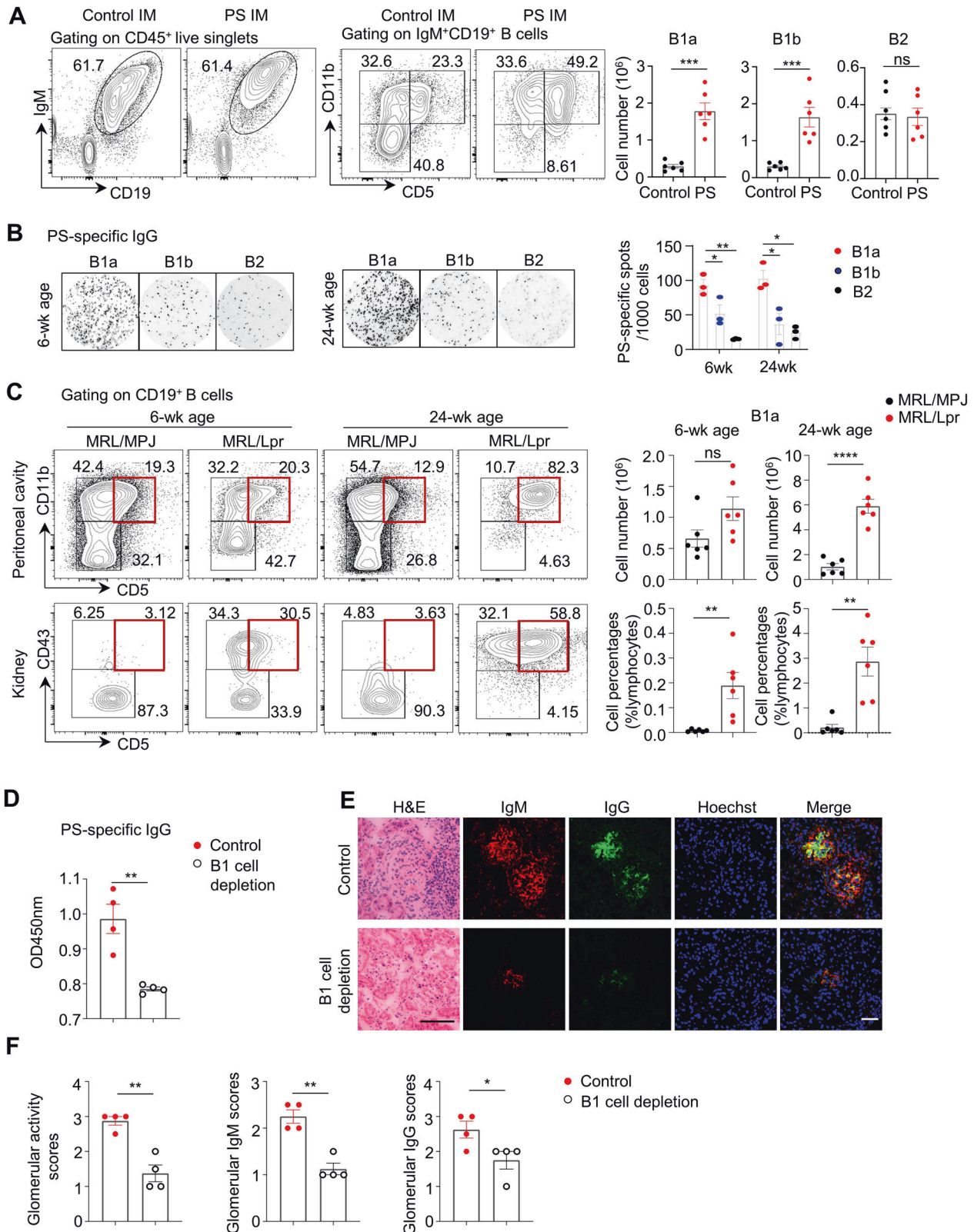


**Fig. 3** B-1 cells are the major source of PS-specific IgG in lupus model mice. **A** Representative flow cytometric profiles and data plots show the B1a cells, B1b cells and B2 cells in peritoneal cavities of control or PS-immunized mice for 12 weeks. **B** Representative ELISPOT detections and data plot show the PS-specific IgG spots in sorting-purified B1a, B1b and B2 cells from peritoneal cavities of MRL/Lpr mice at 6 weeks and 24 weeks of age ( $n = 3$ ). **C** Representative flow cytometric profiles and data plots show B1a cells in peritoneal cavities and kidneys of MRL/MPJ and MRL/Lpr mice at 6 weeks and 24 weeks of age ( $n = 6$  per group). **D** Data plot showing serum PS-specific IgG levels in control or B1-cell-depleted MRL/Lpr mice treated with hypo-osmotic water for 20 successive weeks ( $n = 4$  per group). **E, F** Representative images and plots show H&E, IgM, and IgG staining in kidney sections (scale bar, 20  $\mu$ m) from control or B1a-depleted MRL/Lpr mice ( $n = 4$  per group). One-way ANOVA in **(B)**. Unpaired two-tailed Student's  $t$  test **(A, C, D, F)**, \* $p < 0.05$ ; \*\* $p < 0.01$ ; \*\*\*\* $p < 0.0001$

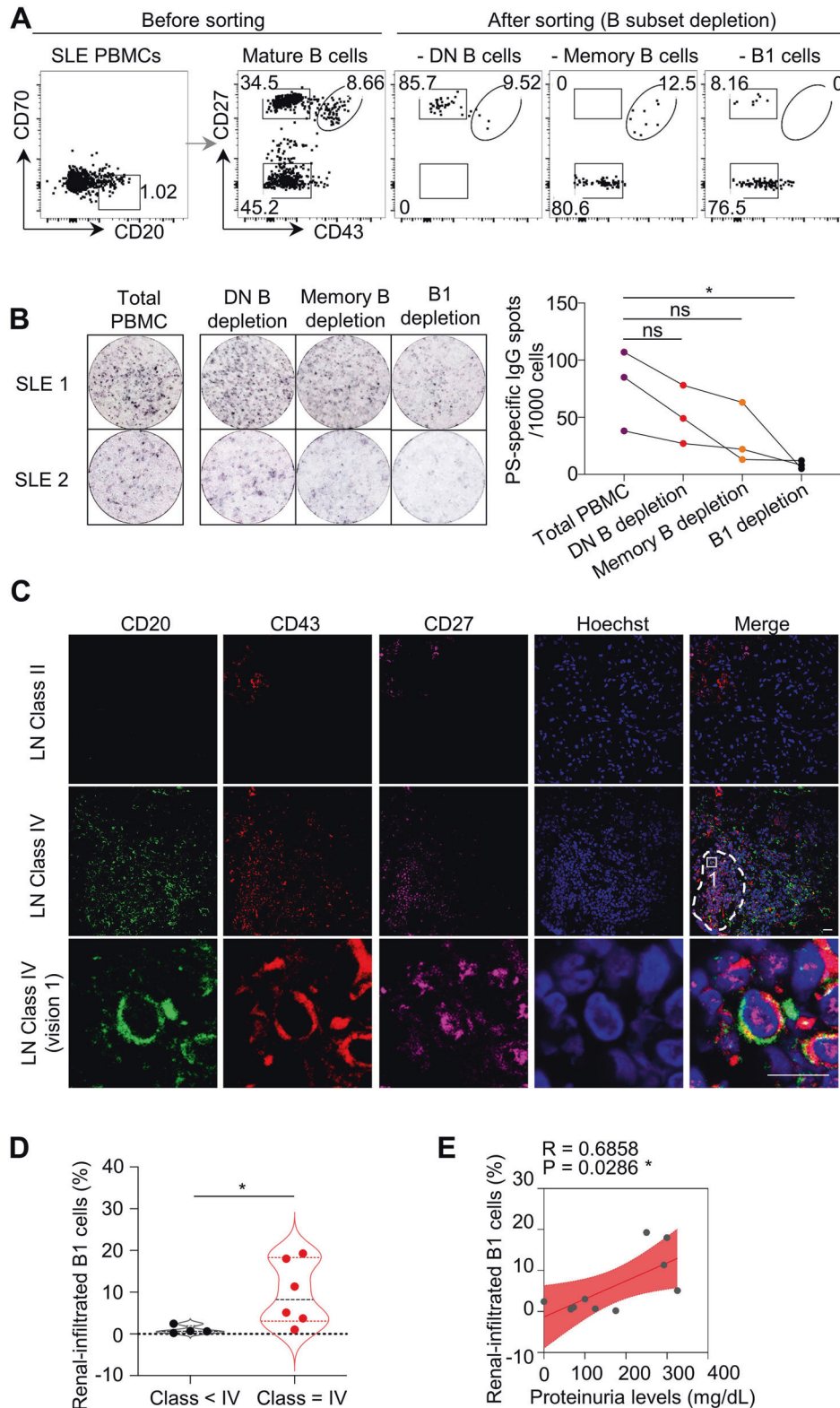


**Fig. 4** B-1 cells are the major source of PS-specific antibodies in SLE patients. **A** Representative flow cytometric profiles show B subsets, including CD27<sup>+</sup>CD43<sup>-</sup> double-negative (DN) B cells, CD27<sup>+</sup>CD43<sup>-</sup> memory B cells, and CD27<sup>+</sup>CD43<sup>+</sup> B1-cell depletion by cell sorting in active SLE PBMCs ( $n = 3$ ). **B** Representative ELISPOT detections and data plot show PS-specific IgG spots in total SLE PBMCs, SLE PBMCs with DN B-cell, memory B-cell or B1-cell depletion ( $n = 3$ ). **C** Representative confocal image shows CD43 (red), CD27 (violet), and CD20 (green) triple-positive B1 cells in kidney biopsies of Class II or Class IV lupus nephritis (LN) patients (scale bar, 20  $\mu$ m). The white dotted box represents the zoomed-in regions for the visualization of confocal images, and the dashed box represents the regions for B1-cell infiltration in kidney biopsies. **D** Data plot shows the distributions of percentages of renal-infiltrated B1 cells in LN patients with Class II–III ( $n = 4$ ) and Class IV ( $n = 6$ ). **E** Plot shows correlation analysis between percentages of renal-infiltrated B1 cells and urine protein levels in LN patients ( $n = 10$ ). One-way ANOVA in **(B)**, nonparametric Mann–Whitney  $U$  test in **(D)** and Spearman's rank correlation analysis in **(E)**; ns no significance; \* $p < 0.05$



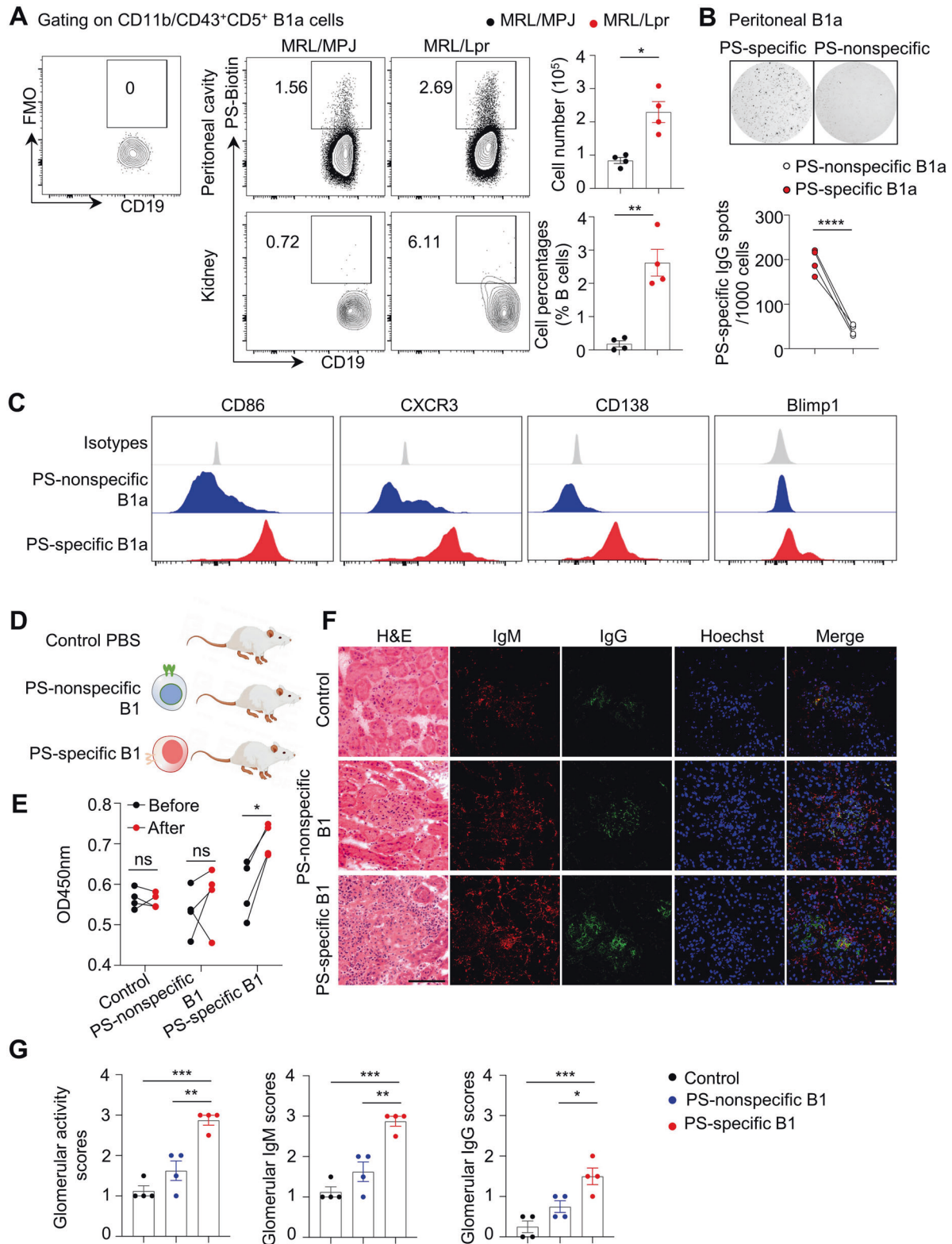


**Fig. 5** Adoptive transfer of PS-specific B-1 cells triggers lupus development in mice. **A** Representative flow cytometric profiles show PS-specific B1a cells in peritoneal cavities and kidneys of MRL/MPJ and MRL/Lpr mice at 24 weeks of age ( $n = 4$  per group). **B** Representative ELISPOT detections and data plot show PS-specific IgG spots in sorting-purified PS-specific and PS-nonspecific B1a cells ( $n = 4$ ). **C** Representative flow cytometric histograms show the expression profiles in PS-specific B1a cells and nonspecific counterparts from peritoneal cavities of MRL/Lpr mice at 24 weeks of age. **D** The schematic diagram shows the 6-week-old MRL/Lpr mice adoptively transferred with PS-specific B1a cells and nonspecific counterparts from 24-week-old MRL/Lpr mice ( $n = 4$  per group). **E** Data plot shows the serum PS-specific IgG levels in recipients before or after cell transfer for 4 weeks by ELISA. **F, G** Representative images and plots show H&E, IgM, and IgG staining in kidney sections (scale bar, 20  $\mu\text{m}$ ) from MRL/Lpr recipients adoptively transferred with PS-specific B1a cells or their nonspecific counterparts for 4 weeks ( $n = 4$  per group). Unpaired two-tailed Student's  $t$  test, \* $p < 0.05$ ; \*\* $p < 0.01$ ; \*\*\* $p < 0.001$ ; \*\*\*\* $p < 0.0001$

specific B1a cells, as detected by ELISPOT assay (Fig. 5B). Flow cytometric analysis showed elevated levels of the costimulatory molecule CD86, chemokine receptor CXCR3, B-cell differentiation markers such as surface CD138 and intranuclear Blimp-1, indicating the functional and differentiation features of PS-specific B1a cells in lupus model mice compared with their PS-nonspecific counterparts (Fig. 5C).

To determine the pathogenic effects of PS-specific B1 cells in lupus nephritis development, we adoptively transferred PS-specific B1a cells and their PS-nonspecific B1a counterparts into MRL/Lpr mice at the disease onset stage (6 weeks old, Fig. 5D). Notably, adoptive transfer of PS-specific B1a cells significantly increased serum levels of PS-specific IgG in lupus recipients at 4 weeks post cell transfer (Fig. 5E). Moreover, compared with PS-nonspecific B1a transfer or control treatment, the transfer of PS-specific B1a cells dramatically accelerated renal damage and glomerular immune complex deposition in 10-week-old lupus recipients (Fig. 5F, G), indicating a pivotal role of PS-specific B1 cells in driving the PS-specific humoral response and renal pathology during lupus development.

### Inhibition of the TLR/Syk signaling pathway suppresses B1-cell expansion and PS-specific IgG production

To determine the molecular mechanisms underlying the expansion of PS-specific B1 cells during lupus development, we examined the expression levels of Toll-like receptors (TLRs) in peritoneal B-cell subsets from lupus model mice. Our data showed elevated mRNA levels of *Tlr8* and *Tlr9* within lupus B1a cells compared with B1b and B2 cells. No significant changes were observed in the expression levels of *Tlr7* transcripts among lupus B1a, B1b, and B2 cells (Fig. 6A). Furthermore, we cultured sorting-purified B1a cells from the peritoneal cavity of 24-week-old MRL/Lpr mice with chromatin components (CCs) extracted from apoptotic cells [29]. In brief, CCs were extracted as nuclear component extracts of ConA-induced activation-induced cell death (AICD) in splenocytes to mimic the accumulation of apoptotic debris during lupus development as previously reported [29]. Notably, CC treatment markedly increased PS-specific IgG-secreting cells and PS-specific subsets in lupus B1a cells by ELISPOT assay and flow cytometry. In addition, DNase I digestion or inhibitory ODN 2088 (TLR7/8/9 antagonist) treatment almost completely abrogated CC-triggered PS-specific IgG autoantibody secretion and PS-specific B1a cell amplification in vitro (Fig. 6B, C).

Furthermore, we treated 6-week-old MRL/Lpr mice with inhibitory ODN 2088 for 4 successive weeks. Comparable numbers and proportions of total B1a cells were observed in MRL/Lpr mice treated with ODN 2088. However, in vivo blockade of TLR7/8/9 signaling with ODN 2088 significantly inhibited peritoneal and renal-infiltrated PS-specific B1a cell expansion in lupus model mice (Fig. 6D).

The tyrosine kinase Syk has been shown to control TLR signal transduction in B cells [30]. We found an ~10-fold increase in the phosphorylation levels of Syk within CC-treated lupus B1a cells. Blockade of TLR signal cascades with DNase I digestion or the inhibitory ODN 2088 dramatically abrogated Syk activation. No significant changes were observed in total Syk levels in lupus B1a cells treated with CC (Fig. 6E). Moreover, the blockade of Syk activation with R406 completely abrogated CC-induced PS-specific IgG secretion in lupus B1a cells (Fig. 6F).

Overall, these results demonstrated a pathological role of chromatin components in triggering the expansion of PS-specific B1 cells and PS-specific autoimmune response via TLR/Syk signal cascades during lupus nephritis development.

### DISCUSSION

Antiphospholipid autoantibodies have been identified in several autoimmune and infectious diseases [6–8], but a direct link

between phospholipid-specific autoantibodies and target organ damage during SLE development remains unclear. In this study, we used various murine lupus models to determine the pathogenic effects of the PS-specific autoimmune response during nephritis development in SLE patients and lupus model mice. In particular, we have shown that B1 cells are the major cellular source for anti-PS antibody production and are critically involved in lupus nephritis progression in vivo. Further mechanistic studies have demonstrated that the TLR/Syk signaling pathway controls the expansion and autoantibody secretion of PS-specific B1a cells. Overall, our findings have identified a novel function of B1-cell-produced anti-PS autoantibodies in mediating nephritis development during the pathogenesis of SLE.

PS-specific IgG has been detected in patients with SLE, APS and systemic sclerosis/scleroderma (SSc) [8, 10, 13, 14]. Recent cohort studies have reported the existence of PS-specific IgG in severe COVID-19 patients [6]. The prevalence of antiphospholipid antibodies (aPL) is associated with thrombosis, pregnancy complications, and neurological disorders in SLE patients [8, 26]. PS-specific autoantibodies also promote the clearance of uninfected erythrocytes and cause anemia in malaria patients [31]. Currently, novel anti-lysobisphosphatidic acid (LBPA) autoantibodies have been reported to generate a self-amplifying autoimmune signal loop during the development of APS and SLE by recognizing a membrane endothelial protein C receptor (EPCR)-LBPA complex and TLR7 signal cascades [11].

Since PS-specific IgG is often excluded from the diagnostic detection of aPL in patients with autoimmune diseases, the functional relevance of PS-specific IgG in lupus pathogenesis remains largely unknown. Herein, we excluded SLE patients with thrombosis or fetal loss to elucidate the role of PS-specific autoantibodies during lupus nephritis development. Compelling evidence indicates that defective clearance of apoptotic cells by macrophage phagocytosis has been observed in SLE patients [32, 33]. Since PS exposure on the cell surface provides key “eat me” signals during apoptotic cell clearance [32], PS-specific IgG may selectively inhibit this process by blocking PS-mediated phagocytic pathways during SLE progression. Here, we show that anti-PS antibodies are deposited in the renal tissue during nephritis development. Moreover, injection of purified PS-specific IgG from SLE serum samples and immunization with PS antigen resulted in renal damage in recipient mice.

B1 cells are derived from distinct precursors and have high expression of surface IgM (sIgM) and CD11b/CD43 in mice. B1 cells are divided into CD5<sup>+</sup> B1a cells and CD5<sup>-</sup> B1b cells [15, 34]. Human B1a cells have been identified in adult peripheral blood with distinct phenotypic markers (CD27<sup>+</sup>CD43<sup>+</sup>CD70<sup>-</sup>) and similar functions as murine B1a cells [21]. B1 cells mainly control T-independent immune responses with natural antibody secretion and self-renewal properties [35]. In lupus-prone MRL/Lpr mice, accumulated autoreactive B1 cells in the peritoneum are coincident with lupus development. Adoptive transfer of peritoneal cells accelerates lupus development and autoimmune response [36]. Lupus-prone NZB/NZW F1 mice exhibited significant expansion of B1a cells [37]. Elimination of B1 cells in the peritoneum has been reported as an effective therapeutic approach for the treatment of SLE in lupus-prone NZB/NZW F1 mice as evidenced by decreased anti-DNA IgG antibodies in the sera and reduced pathological changes in the kidneys [37, 38]. Importantly, robust amplification of CD11b<sup>+</sup> B1 cells with elevated levels of surface CD86 expression has been identified in the peripheral blood of SLE patients [22], indicating a pathogenic role of B1 cells during lupus development [39]. Although we have identified B1 cells as the main cell source of anti-PS IgG during murine lupus development, further investigation is needed to determine whether endogenous PS-specific IgG expression in B1 cells is also upregulated in both lupus model mice and SLE patients.

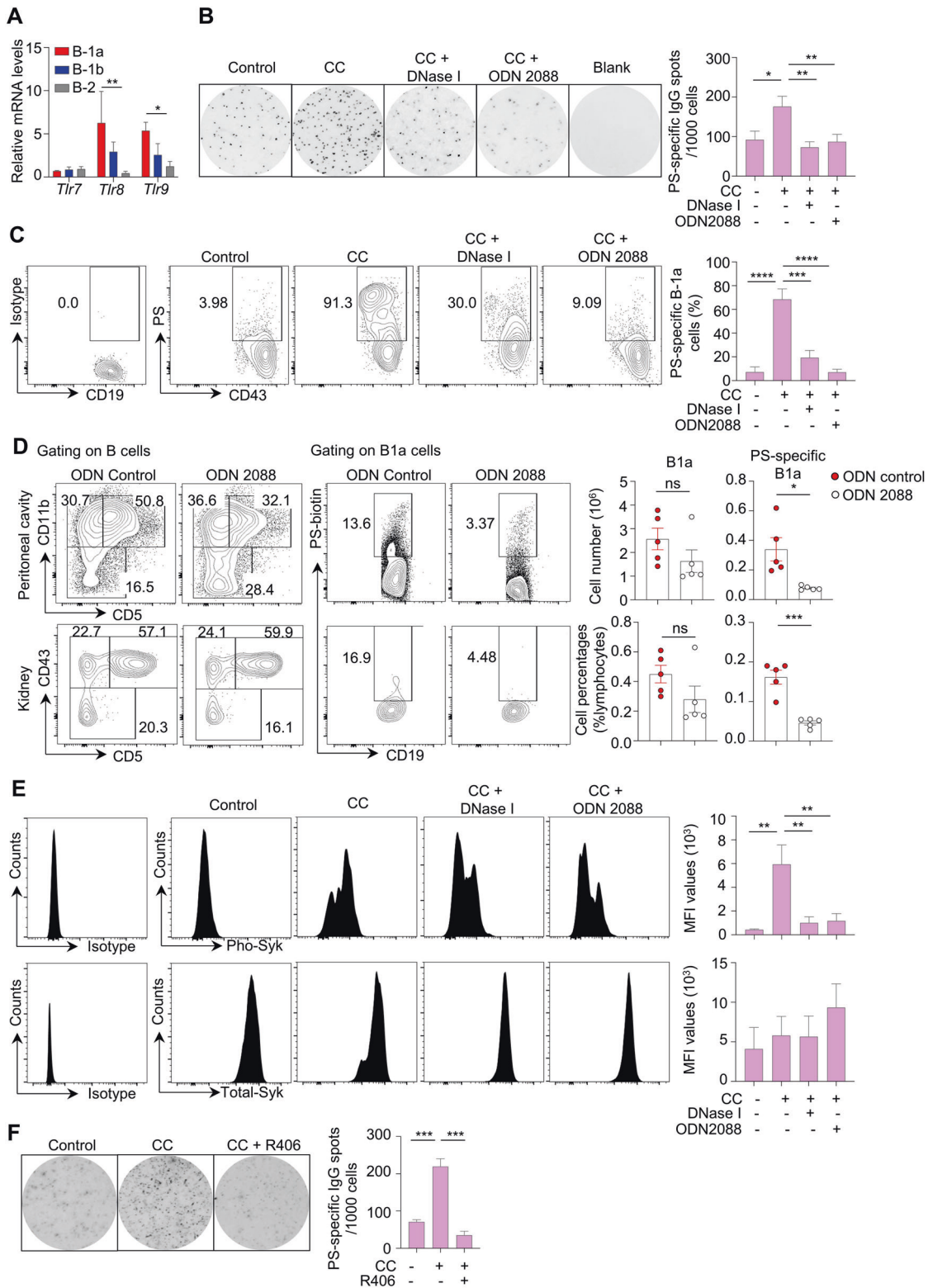


**Fig. 6** Chromatin components control PS-specific B-1 cell expansion in vitro via TLR/Syk activation. **A** Bar plot showing the relative mRNA levels of *Tlr7*, *Tlr8*, and *Tlr9* in sorting-purified B1a cells, B1b cells and B2 cells from the peritoneal cavities of 24-week-old MRL/Lpr mice ( $n = 3$ ). **B**, **C** Representative ELISPOT detections, flow cytometric profiles and data plots show PS-specific IgG spots and PS-specific B1a cells in sorting-purified B1a cells with CpG ODN, chromatin components (CCs), CCs combined with DNase I and CCs combined with inhibitory ODN 2088 treatment for 48 h. **D** Representative flow cytometric profiles and data plots show total and PS-specific B1a cells in peritoneal cavities and kidneys of MRL/Lpr mice with control ODN or inhibitory ODN2088 treatment for 4 successive weeks ( $n = 5$  per group). **E** Representative flow cytometric histograms and data plots show phosphorylated (Pho)-Syk and total Syk levels by phosphorylated flow cytometry in sorting-purified B1a cells treated with CC alone or combined with either DNase I or ODN2088 for 48 h ( $n = 4$ ). **F** Representative ELISPOT detections and data plot show PS-specific IgG spots in sorting-purified B1a cells treated with CC or CC combined with the Syk inhibitor R406 for 48 h ( $n = 4$ ). One-way ANOVA (**A–C**, **E**, **F**) and unpaired two-tailed Student's *t* test in (**D**); ns no significance; \* $p < 0.05$ ; \*\* $p < 0.01$ ; \*\*\* $p < 0.001$

B1a cell depletion also ameliorated collagen-induced arthritis (CIA) development in mice [40]. However, an atypical memory B-cell subset with FCRL5 and T-bet expression showed high specificities to the exposed PS in erythrocytes [41]. Herein, we observed the B1-cell-dominated PS-specific autoimmune response in SLE patients and lupus model mice, indicating the disease- or pathogen-specific autoimmune response against phospholipid antigens.

The homing, migration, and organ distribution of B1a cells are closely controlled by chemokine signals [15]. B1 cells highly express CXCR5, the chemokine receptor for CXCL13. Significantly impaired B-cell populations and failed body-cavity homing of B1 cells have been observed in mice with CXCL13 deficiency [36]. Defective B1-cell homing toward the body cavity and preferential recruitment to the damaged kidneys have been shown in lupus-prone NZB/NZW F1 mice with reduced CXCL13 expression levels during disease progressive stages [37]. Moreover, ligation of TLRs specifically induces the transient downregulation of surface integrins on B1 cells and controls the detachment of B1 cells from the local matrix in body cavities [42]. Here, our phenotypic analysis revealed elevated surface CXCR3 expression levels in PS-specific B1a cells and renal infiltration of B1a cells in lupus model mice, demonstrating the distinct migration features of PS-specific B1a cells in SLE. Further investigations are needed to characterize the functional and phenotypic features of human PS-specific B1 cells from SLE patients.

Approximately 7% of peritoneum B1 cells are specific for phosphatidylcholine (PtC), a common membrane phospholipid in eukaryotes and bacteria [42]. Previous studies have indicated that PtC-binding BCRs with self-reactivity are predominantly encoded by VH11/JH1 and VH12/JH1 in C57BL/6 mice and by VHQ52/JH4 in BALB/c mice [43]. Interestingly, previous studies have applied heavy chain (H) editing by replacing an arginine (Arg) residue with glycine (Gly) in the VH region of the anti-dsDNA antibody to reverse the antibody affinity, which leads to dramatically reduced antibody affinity for dsDNA but enhanced affinity for the PS antigen [44]. Here, we analyzed PS-specific and dsDNA-specific IgG-secreting cells in the spleen and peritoneal cavity of lupus-prone mice at the disease onset stage and observed that the PS-specific B-cell response was mainly restricted to peritoneal B cells rather than spleen B cells. These results indicate the dominant role of the peritoneal B1-cell-mediated PS-specific autoimmune response in lupus model mice. Thus, further studies on B-cell repertoire sequencing and antibody affinity analysis are needed to characterize lupus PS-specific B1a cells.

Increasing evidence indicates that TLR-mediated signals control the migration and function of B1a cells [42]. TLR7, TLR8 and TLR9 are evolutionarily conserved receptors for microbial or endogenous nucleic acids and are closely involved in SLE development [45]. In lupus model mice, TLR7 deficiency ameliorated disease development, but TLR8 or TLR9 deficiency exacerbated SLE symptoms [46]. Interestingly, the TLR7-mediated autoimmune response is controlled by TLR8 signaling in dendritic cells and TLR9 signaling in B cells [47]. Importantly, a gain-of-function variant of TLR7<sup>Y264H</sup> selectively promoted aberrant survival of BCR-activated B cells and CD11c<sup>+</sup> age-associated B-cell generation during human lupus pathogenesis [48]. It has been reported that B-cell-intrinsic TLR9 signaling plays a protective role in murine lupus [49]. Intriguingly, paired immunoglobulin (Ig)-like receptor B (PIR-B) restrains TLR9 signal activation in B1 cells and ameliorates lupus progression in MRL/Lpr mice [50]. In lupus-prone female and male B6.Nba2. Yaa mice, deletion of *Tlr8* accelerated disease progression and mortality, accompanied by increased levels of serum anti-nuclear autoantibodies (ANAs) and increased surface MHCII levels in B cells that enhanced monocyte activation. The accelerated disease progression in TLR8-deficient lupus model mice might depend on TLR7 activation [46]. Moreover, the expansion of B1a cells is tightly modulated by certain transcription factors, including Bhlhe41 and Ikaros [51, 52]. Herein, we observed

that apoptotic cell-derived chromatin components robustly trigger PS-specific B1a cell proliferation and autoantibody secretion, whereas blockade of TLR7/8/9 or elimination of DNA antigens significantly reduced the expansion of PS-specific B1a cells in culture and in lupus model mice. Since it has been shown that synthetic G-rich DNA, known to block CpG-DNA effects, can inhibit TLR-9-mediated immunostimulatory effects and ameliorate murine lupus development [53], further investigations are needed to examine the distinct roles of TLR signals in the B1-cell response and the underlying mechanisms during lupus development.

Recent studies have revealed that spleen tyrosine kinase (Syk), a cytoplasmic protein tyrosine kinase, is predominantly expressed in cells of the hematopoietic lineage [30]. Entospletinib (GS-9973), an oral selective inhibitor of Syk, shows clinical efficacy in subjects with relapsed or refractory chronic lymphocytic leukemia (CLL) [54]. Syk-dependent signaling is initiated at the plasma membrane for TLR-induced B-cell proliferation and differentiation by crosstalk with B-cell receptor pathways [55]. Interestingly, B lymphoid tyrosine kinase (BLK), a Syk-associated kinase, has also been shown to control the expansion of B1 cells in lupus patients and mouse models [54]. Further studies may provide new insight into the crucial role of Syk signaling activation in the enhanced B1 response and autoantibody production in autoimmune pathogenesis.

In summary, we have shown that PS-specific autoantibodies are predominantly produced by B1 cells in SLE patients and lupus model mice. Moreover, anti-PS autoantibodies are involved in the development of lupus nephritis and their secretion is modulated by the activation of the TLR/Syk signaling cascade. In this study, we provide evidence that the PS-specific B1-cell-mediated autoimmune response not only serves as a diagnostic marker for SLE but also plays a key pathogenic role in the initiation and exacerbation of lupus nephritis. These findings suggest that B1-cell depletion and blockade of TLR/Syk activation may represent potential strategies for the treatment of LN and other autoimmune diseases.

## REFERENCES

- Zhao Z, Ren J, Dai C, Kannapell CC, Wang H, Gaskin F, et al. Nature of T cell epitopes in lupus antigens and HLA-DR determines autoantibody initiation and diversification. *Ann Rheum Dis.* 2019;78:380–90.
- Ma K, Du W, Xiao F, Han M, Huang E, Peng N, et al. IL-17 sustains the plasma cell response via p38-mediated Bcl-xL RNA stability in lupus pathogenesis. *Cell Mol Immunol.* 2021;18:1739–50.
- Zhao Z, Xu B, Wang S, Zhou M, Huang Y, Guo C, et al. Tfh cells with NLRP3 inflammasome activation are essential for high-affinity antibody generation, germinal centre formation and autoimmunity. *Ann Rheum Dis.* 2022;81:1006–12.
- Waters ST, McDuffie M, Bagavant H, Deshmukh US, Gaskin F, Jiang C, et al. Breaking tolerance to double stranded DNA, nucleosome, and other nuclear antigens is not required for the pathogenesis of lupus glomerulonephritis. *J Exp Med.* 2004;199:255–64.
- Fu SM, Dai C, Zhao Z, Gaskin F. Anti-dsDNA antibodies are one of the many autoantibodies in systemic lupus erythematosus. *F1000Res.* 2015;4:939.
- Zuo Y, Estes SK, Ali RA, Gandhi AA, Yalavarthi S, Shi H, et al. Prothrombotic autoantibodies in serum from patients hospitalized with COVID-19. *Sci Transl Med.* 2020;12:eabd3876.
- Tselios K, Sarantopoulos A, Gkoukourellas I, Boura P. The role of anti-phosphatidylserine/prothrombin antibodies in thrombotic manifestations of systemic lupus erythematosus patients. *Front Neurol.* 2013;4:66.
- Radin M, Cecchi I, Rubini E, Schreiber K, Roccatello D, Mahler M, et al. Prevalence and significance of anti-phosphatidylserine antibodies: a pooled analysis in 5992 patients. *Thromb Res.* 2018;170:28–31.
- Zhu H, Luo H, Yan M, Zuo X, Li QZ. Autoantigen microarray for high-throughput autoantibody profiling in systemic lupus erythematosus. *Genomics Proteomics Bioinformatics.* 2015;13:210–18.
- Farina N, Abdulsalam R, McDonnell T, Pericleous C, D'Souza A, Ripoll VM, et al. Antiphospholipid antibody positivity in early systemic lupus erythematosus is associated with subsequent vascular events. *Rheumatology.* 2022;62:2252–6.
- Muller-Calleja N, Hollerbach A, Royce J, Ritter S, Pedrosa D, Madhusudhan T, et al. Lipid presentation by the protein C receptor links coagulation with autoimmunity. *Science.* 2021;371:eabc0956.

12. Sprangers B, Monahan M, Appel GB. Diagnosis and treatment of lupus nephritis flares-an update. *Nat Rev Nephrol.* 2012;8:709–17.
13. Fischer K, Przepiera-Bedzak H, Brzosko I, Sawicki M, Walecka A, Brzosko M. Anti-phosphatidylethanolamine and anti-phosphatidylserine antibodies-association with renal involvement, atherosclerosis, cardiovascular manifestations, Raynaud phenomenon and disease activity in Polish patients with systemic lupus erythematosus. *Biomolecules.* 2022;12:1328.
14. Sawada T, Kurano M, Shirai H, Iwasaki Y, Tahara K, Hayashi H, et al. Serum phosphatidylserine-specific phospholipase A1 as a novel biomarker for monitoring systemic lupus erythematosus disease activity. *Int J Rheum Dis.* 2019;22:2059–66.
15. Baumgarth N. The double life of a B-1 cell: self-reactivity selects for protective effector functions. *Nat Rev Immunol.* 2011;11:34–46.
16. Wang X, Ma K, Chen M, Ko KH, Zheng BJ, Lu L. IL-17A promotes pulmonary B-1a cell differentiation via induction of Blimp-1 Expression During Influenza Virus Infection. *PLoS Pathog.* 2016;12:e1005367.
17. Yang Y, Li X, Ma Z, Wang C, Yang Q, Byrne-Steele M, et al. CTLA-4 expression by B-1a B cells is essential for immune tolerance. *Nat Commun.* 2021;12:525.
18. Xu Z, Butfiloski EJ, Sobel ES, Morel L. Mechanisms of peritoneal B-1a cells accumulation induced by murine lupus susceptibility locus Sle2. *J Immunol.* 2004;173:6050–8.
19. Duan B, Morel L. Role of B-1a cells in autoimmunity. *Autoimmun Rev.* 2006;5:403–8.
20. Diana J, Simoni Y, Furio L, Beaudoin L, Agerberth B, Barrat F, et al. Crosstalk between neutrophils, B-1a cells and plasmacytoid dendritic cells initiates autoimmune diabetes. *Nat Med.* 2013;19:65–73.
21. Griffin DO, Holodick NE, Rothstein TL. Human B1 cells in umbilical cord and adult peripheral blood express the novel phenotype CD20+ CD27+ CD43+ CD70. *J Exp Med.* 2011;208:67–80.
22. Griffin DO, Rothstein TL. A small CD11b(+) human B1 cell subpopulation stimulates T cells and is expanded in lupus. *J Exp Med.* 2011;208:2591–8.
23. Ma K, Wang X, Shi X, Lin X, Xiao F, Ma X, et al. The expanding functional diversity of plasma cells in immunity and inflammation. *Cell Mol Immunol.* 2020;17:421–2.
24. Ma K, Li J, Wang X, Lin X, Du W, Yang X, et al. TLR4(+)-CXCR4(+) plasma cells drive nephritis development in systemic lupus erythematosus. *Ann Rheum Dis.* 2018;77:1498–506.
25. Wu L, Seon GM, Kim Y, Choi SH, Vo QC, Yang HC. Enhancing effect of sodium butyrate on phosphatidylserine-liposome-induced macrophage polarization. *Inflamm Res.* 2022;71:641–52.
26. Petri M, Orbai AM, Alarcon GS, Gordon C, Merrill JT, Fortin PR, et al. Derivation and validation of the systemic lupus international collaborating clinics classification criteria for systemic lupus erythematosus. *Arthritis Rheum.* 2012;64:2677–86.
27. Fukushi S. Competitive ELISA for the detection of serum antibodies specific for middle east respiratory syndrome coronavirus (MERS-CoV). *Methods Mol Biol.* 2020;2203:55–65.
28. Hu K. Become competent within one day in generating boxplots and violin plots for a novice without prior R experience. *Methods Protoc.* 2020;3:64.
29. Li H, Zhang YY, Sun YN, Huang XY, Jia YF, Li D. Induction of systemic lupus erythematosus syndrome in BALB/c mice by immunization with active chromatin. *Acta Pharm Sin.* 2004;25:807–11.
30. Alsadeq A, Hobeika E, Medgyesi D, Klasener K, Reth M. The role of the Syk/Shp-1 kinase-phosphatase equilibrium in B cell development and signaling. *J Immunol.* 2014;193:268–76.
31. Fernandez-Arias C, Rivera-Correa J, Gallego-Delgado J, Rudlaff R, Fernandez C, Roussel C, et al. Anti-self phosphatidylserine antibodies recognize uninfected erythrocytes promoting malarial anemia. *Cell Host Microbe.* 2016;19:194–203.
32. Nagata S. Apoptosis and clearance of apoptotic cells. *Annu Rev Immunol.* 2018;36:489–517.
33. Qian Y, Conway KL, Lu X, Seitz HM, Matsushima GK, Clarke SH. Autoreactive MZ and B-1 B-cell activation by Faspr is coincident with an increased frequency of apoptotic lymphocytes and a defect in macrophage clearance. *Blood.* 2006;108:974–82.
34. Berland R, Wortis HH. Origins and functions of B-1 cells with notes on the role of CD5. *Annu Rev Immunol.* 2002;20:253–300.
35. Clarke AJ, Riffelmacher T, Braas D, Cornell RJ, Simon AK. B1a B cells require autophagy for metabolic homeostasis and self-renewal. *J Exp Med.* 2018;215:399–413.
36. Ansel KM, Harris RB, Cyster JG. CXCL13 is required for B1 cell homing, natural antibody production, and body cavity immunity. *Immunity.* 2002;16:67–76.
37. Ito T, Ishikawa S, Sato T, Akadegawa K, Yurino H, Kitabatake M, et al. Defective B1 cell homing to the peritoneal cavity and preferential recruitment of B1 cells in the target organs in a murine model for systemic lupus erythematosus. *J Immunol.* 2004;172:3628–34.
38. Murakami M, Yoshioka H, Shirai T, Tsubata T, Honjo T. Prevention of autoimmune symptoms in autoimmune-prone mice by elimination of B-1 cells. *Int Immunol.* 1995;7:877–82.
39. Wu YY, Georg I, Diaz-Barreiro A, Varela N, Lauwerys B, Kumar R, et al. Concordance of increased B1 cell subset and lupus phenotypes in mice and humans is dependent on BLK expression levels. *J Immunol.* 2015;194:5692–702.
40. Deng J, Wang X, Chen Q, Sun X, Xiao F, Ko KH, et al. B1a cells play a pathogenic role in the development of autoimmune arthritis. *Oncotarget.* 2016;7:19299–311.
41. Rivera-Correa J, Mackroth MS, Jacobs T, Schulze Zur Wiesch J, Rolling T, Rodriguez A. Atypical memory B-cells are associated with Plasmodium falciparum anemia through anti-phosphatidylserine antibodies. *Elife.* 2019;8:e48309.
42. Ha SA, Tsuji M, Suzuki K, Meek B, Yasuda N, Kaisho T, et al. Regulation of B1 cell migration by signals through Toll-like receptors. *J Exp Med.* 2006;203:2541–50.
43. Seidl KJ, Wilshire JA, MacKenzie JD, Kantor AB, Herzenberg LA, Herzenberg LA. Predominant VH genes expressed in innate antibodies are associated with distinctive antigen-binding sites. *Proc Natl Acad Sci USA.* 1999;96:2262–7.
44. Li H, Jiang Y, Cao H, Radic M, Prak EL, Weigert M. Regulation of anti-phosphatidylserine antibodies. *Immunity.* 2003;18:185–92.
45. Ma K, Li J, Fang Y, Lu L. Roles of B cell-intrinsic TLR signals in systemic lupus erythematosus. *Int J Mol Sci.* 2015;16:13084–105.
46. Tran NL, Manzin-Lorenzi C, Santiago-Raber ML. Toll-like receptor 8 deletion accelerates autoimmunity in a mouse model of lupus through a Toll-like receptor 7-dependent mechanism. *Immunology.* 2015;145:60–70.
47. Desnues B, Macedo AB, Roussel-Queval A, Bonnardel J, Henri S, Demaria O, et al. TLR8 on dendritic cells and TLR9 on B cells restrain TLR7-mediated spontaneous autoimmunity in C57BL/6 mice. *Proc Natl Acad Sci USA.* 2014;111:1497–502.
48. Brown GJ, Canete PF, Wang H, Medhavy A, Bones J, Roco JA, et al. TLR7 gain-of-function genetic variation causes human lupus. *Nature.* 2022;605:349–56.
49. Wu X, Peng SL. Toll-like receptor 9 signaling protects against murine lupus. *Arthritis Rheum.* 2006;54:336–42.
50. Kubo T, Uchida Y, Watanabe Y, Abe M, Nakamura A, Ono M, et al. Augmented TLR9-induced Btk activation in PIR-B-deficient B-1 cells provokes excessive autoantibody production and autoimmunity. *J Exp Med.* 2009;206:1971–82.
51. Kreslavsky T, Vilagos B, Tagoh H, Poliakova DK, Schwickert TA, Wohner M, et al. Essential role for the transcription factor Bhlhe41 in regulating the development, self-renewal and BCR repertoire of B-1a cells. *Nat Immunol.* 2017;18:442–55.
52. Macias-Garcia A, Heizmann B, Sellars M, Marchal P, Dali H, Pasquali JL, et al. Ikaros is a negative regulator of B1 cell development and function. *J Biol Chem.* 2016;291:9073–86.
53. Patole PS, Zecher D, Pawar RD, Grone HJ, Schlondorff D, Anders HJ. G-rich DNA suppresses systemic lupus. *J Am Soc Nephrol.* 2005;16:3273–80.
54. Burke JM, Shustov A, Essell J, Patel-Donnelly D, Yang J, Chen R, et al. An open-label, phase II trial of entospletinib (GS-9973), a selective spleen tyrosine kinase inhibitor, in diffuse large B-cell lymphoma. *Clin Lymphoma Myeloma Leuk.* 2018;18:e327–31.
55. Schweighoffer E, Nys J, Vanes L, Smithers N, Tybulewicz VJL. TLR4 signals in B lymphocytes are transduced via the B cell antigen receptor and SYK. *J Exp Med.* 2017;214:1269–80.

## ACKNOWLEDGEMENTS

We thank Dr. Kwok Wah Chan, Dr. Xi Yang, and Mr. King-Hung Ko for their kind help in the renal histopathological assessment and technical assistance. We also thank the service of the Medical Faculty Core Facility and Laboratory Animal Unit, The University of Hong Kong.

## AUTHOR CONTRIBUTIONS

KM, WD, SW, and JT designed and performed the mouse experiments and statistical analysis. JL, YX, XZ, JW, CL, HW, and FX performed the experiments with human samples. XK, KR, QR, HZ, YZ, CW, DL, and LH participated in the data analysis. LL, QL, and LW supervised the study, and KM wrote the manuscript.

## FUNDING

This work was supported by funding for Chongqing International Institute for Immunology (2020YJC10), National Natural Science Foundation of China (81901635, 82171782, 82260326, 81971464), Shenzhen Science and Technology Program (CYJ20210324114602008), Hong Kong Research Grants Council Theme-Based Research Scheme (T12-703/19R) and the Centre for Oncology and Immunology under the Health@InnoHK Initiative by the Innovation and Technology Commission, Hong Kong, China.

## COMPETING INTERESTS

The authors declare no competing interests.

**ETHICAL APPROVAL**

All human experiments were approved by the Institutional Medical Ethics Committee of Third Military Medical University (Reference Number: 2016-77-tmmu) and Institutional Review Board of the University of Hong Kong/Hospital Authority Hong Kong Western Cluster (HKU/HA HKW IRB) (Reference Number: UW 16-342). Written permission was obtained from all subjects who participated in the study. All animal experiments were approved by the Committee on the Use of Live Animals in Teaching and Research (CULATR, No: 3392-14) at the University of Hong Kong.

**ADDITIONAL INFORMATION**

**Supplementary information** The online version contains supplementary material available at <https://doi.org/10.1038/s41423-023-01049-2>.

**Correspondence** and requests for materials should be addressed to Qianjin Lu, Lijun Wu or Liwei Lu.

**Reprints and permission information** is available at <http://www.nature.com/reprints>

Springer Nature or its licensor (e.g. a society or other partner) holds exclusive rights to this article under a publishing agreement with the author(s) or other rightsholder(s); author self-archiving of the accepted manuscript version of this article is solely governed by the terms of such publishing agreement and applicable law.